

Solid-state microscale lithium batteries prepared with microfabrication processes

This content has been downloaded from IOPscience. Please scroll down to see the full text.

2009 J. Micromech. Microeng. 19 045004

(<http://iopscience.iop.org/0960-1317/19/4/045004>)

View [the table of contents for this issue](#), or go to the [journal homepage](#) for more

Download details:

IP Address: 59.77.43.191

This content was downloaded on 12/07/2015 at 03:26

Please note that [terms and conditions apply](#).

Solid-state microscale lithium batteries prepared with microfabrication processes

Jie Song¹, Xi Yang¹, Shuang-Shuang Zeng¹, Min-Zhen Cai²,
Liang-Tang Zhang², Quan-Feng Dong^{1,5}, Ming-Sen Zheng¹, Sun-Tao Wu³
and Qi-Hui Wu^{4,5}

¹ State Key Laboratory for Physical Chemistry of Solid Surfaces and Department of Chemistry, Xiamen University, Xiamen 361005, People's Republic of China

² Department of Physics, Xiamen University, Xiamen 361005, People's Republic of China

³ Pen Tung Sah MEMS Research Center, Xiamen University, Xiamen 361005, People's Republic of China

⁴ Department of Physics, La Trobe University, Bundoora 3086, VIC, Australia

E-mail: qfdong@xmu.edu.cn and q.wu@latrobe.edu.au

Received 5 December 2008, in final form 27 January 2009

Published 11 March 2009

Online at stacks.iop.org/JMM/19/045004

Abstract

The miniaturization of power sources is important for meeting the requirements of low power, mass and volume for nano- or microelectronics and MEMS devices. In this paper a dexterous microfabrication process was developed for preparing microscale solid-state lithium batteries. The active size of a single microbattery is $500\ \mu\text{m} \times 500\ \mu\text{m}$ and its thickness is $1.5\ \mu\text{m}$. LiCoO_2 films prepared by RF sputtering, then annealed at moderate temperature ($500\ ^\circ\text{C}$), were employed as a cathode electrode, and LiPON and Al films were used as a solid electrolyte and an anode electrode, respectively. An individual microbattery delivers a capacity of about 17 nAh at a current of 5 nA at the initial cycles, and can be operated at as high as 40 nA discharge current.

1. Introduction

Most low-power electronic and microelectronmechanical system (MEMS) devices designed today use conventionally macroscopic external power supplies. This places limits on the functionality of these microdevices in many applications. An alternative solution is to design power sources at a microscale, which can be integrated together with these microdevices on the same chips [1]. There are various microbatteries reported in the literature as power supplies for microdevices. Sammoura *et al* [2] reported the water-activated microbatteries with magnesium and silver chloride as the anode and cathode electrodes, which have great potential to be integrated with microdevices for diagnostics and BioMEMS chips. Chamran *et al* [3] presented a series of microfabrication procedures to fabricate nickel–zinc batteries with three-dimensional (3D) structures. Moreover, fuel cells and semi-fuel cells with miniaturized dimensions have also been fabricated [4–7]. An all solid-state microscale lithium battery is also a good choice

as a micropower source [8] due to several advantages it has, such as significant reductions in the mass, self-operation and good endurance to adverse environmental conditions. A large body of research has been performed on the study of battery component materials and thin-film lithium batteries [9–15]. Typically, thin-film lithium batteries were fabricated with physical masks, which do not allow the sizes of batteries below several tens of mm^2 and are hard to be integrated with microdevices [16–20]. Few reports were concerned with the miniaturization of lithium batteries using microfabrication techniques. This may be due, in part, to the significant difficulties associated with the microfabrication and testing of the microbatteries, including water-sensitive materials. In 2002, West's group [21] first reported the fabrication and testing of all solid-state microscale lithium batteries. Photolithography, sputtering as well as ionic dry etching were employed in the preparation of Li-free structure microscale batteries with active areas of the order of $(50\text{--}100\ \mu\text{m})^2$. Nickel film with lithium *in situ* planted on it was used as a block electrode and anode. These cells could discharge at 3.9 V with an initial capacity of about 1 nAh, but faded

⁵ Author to whom any correspondence should be addressed

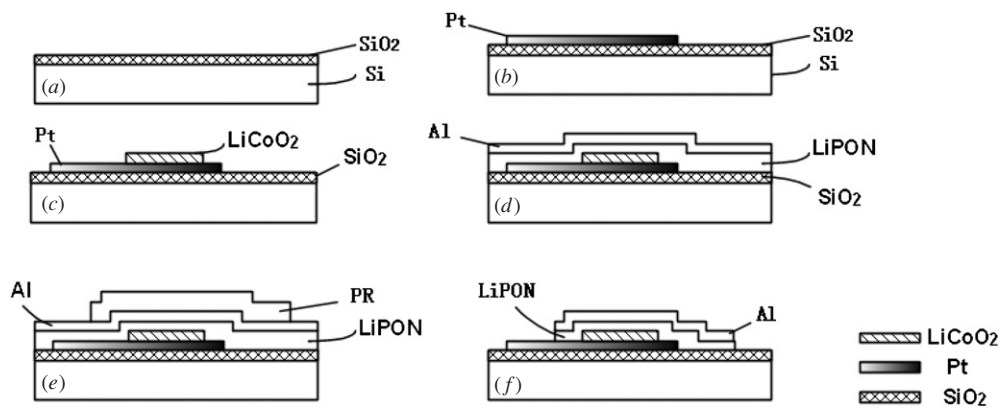


Figure 1. Schematic process for fabrication of microbatteries.

to 20% of the initial capacity after five cycles. This is probably because the *in situ* planted lithium metal gradually becomes electrochemically inactive under exposure of O_2 and H_2O [22]. In 2003, the same group [23] reported another fabrication process of microbatteries using Li metal as the anode, but this process was complicated and the LiPON layer was exposed to an aqueous solution and air during processing. Recently Baggetto *et al* [24, 25] proposed an interesting concept of micro-lithium batteries with a 3D structure. In this structure, an anisotropic etched Si with a large surface area was used as the substrate. The active layers could then be deposited inside the high-aspect-ratio structured substrate using the step-conformal deposition technologies, such as low-pressure chemical vapor deposition (LPCVD) and atomic layer deposition (ALD). However, the deposition of solid electrolyte and cathode materials by LPCVD and ALD is still challenging. Using the common deposition techniques such as radio frequency (RF) sputtering or pulse laser deposition (PLD) it is difficult to deposit homogenous layers in the high-aspect-ratio structure. Unfortunately, the authors did not report the solution of the above challenges and the electrochemical results of the 3D structure microbatteries.

In this study a dexterous microfabrication process of Li microbatteries is presented including photolithography, magnetron sputtering and wet etching techniques. $LiCoO_2$ films were used as the cathode electrode, and LiPON films as the electrolyte. Because the etching process of Al films is mature in the microelectronic industry, and Al films could alloy/dealloy with Li by electrochemical reactions [26, 27], these films were selected as the anode electrode as well as protective coating layers. The microbatteries reported in this work can avoid the use of reactive metallic lithium anodes, which requires expensive packaging technology and cannot endure the re-flow soldering process.

2. Experimental details

2.1. Fabrication

All the components of microbatteries were deposited by the conventional JC500-3/D RF magnetron sputtering system. The $LiCoO_2$ and Li_3PO_4 targets were purchased from STMC, USA. The photolithography was carried out using a

Karlsruh MA6/BA6 mask aligner. The fabrication process of microbatteries is schematically represented in figure 1. The whole process was performed in a clean room environment. On a 2 inch silicon wafer, a 500 nm thick silicon dioxide film was grown by thermal oxidation as an insulating layer between the microbatteries (figure 1(a)). It was then patterned with image reversal photoresist (AZ 5214E, MicroChemicals GmbH) to define the current collector. After a 10 nm thick Ti adhesion film and a 300 nm thick Pt film were deposited on the patterned photoresist, the Si wafer was then immersed in acetone to remove the photoresist and tear off the excess Ti/Pt film (figure 1(b)). To define the microbatteries cathodes, the substrates were again patterned with reversal photoresist, yielding square openings in the photoresist with the area of $500 \mu m \times 500 \mu m$ over the cathode current collectors. $LiCoO_2$ films were sputtered over the photoresist, and the substrates were then immersed in acetone to remove the photoresist and lift off the excess $LiCoO_2$ films (figure 1(c)). Following patterning of the $LiCoO_2$ feature, the substrate was treated with an annealing process at $500^\circ C$ for 1 h in O_2 atmosphere to decrease lattice strain and enhance the crystallization of as-deposited $LiCoO_2$ films. The solid-state electrolyte LiPON was then deposited over the cathode electrode with a thickness of 600–900 nm. Finally, the Al anode films were subsequently deposited on the LiPON film by direct current magnetron sputtering (figure 1(d)). The wafer was removed from the sputtering chamber and patterned with positive photoresist (BP-212, Beijing Institute of Chemical Reagent) for etching to define the Al and electrolyte films (figure 1(e)). The Al and electrolyte films were etched with a solution of $H_3PO_4:HNO_3:HAc:H_2O$ at a ratio of 16:1:1:2. Afterward, the photoresist was removed with acetone yielding the full microbattery structure (figure 1(f)).

2.2. Packing and testing

Approximately 800 individual microbattery cells per 2 inch wafer were fabricated at the same time. Following the cells separation by diamond saw, the cells were attached on semiconductor device bases, and then were connected with external circuits using ultrasonic bonding with an aluminum wire. The metallic protective caps were placed over the microbatteries, and the devices were then sealed by epoxy

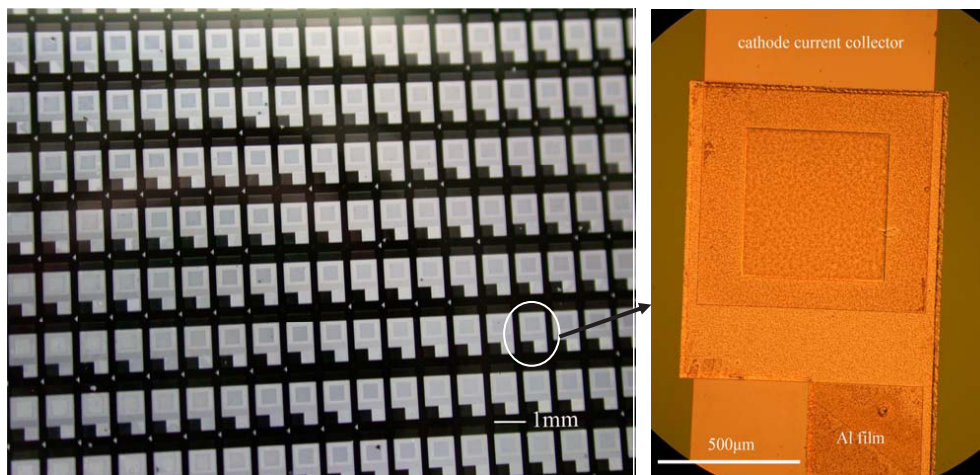


Figure 2. The optical photograph of microfabricated batteries on the 2 inch Si wafer.

in the glovebox. The cells were charged and discharged using a Perkin-Elmer 273A potentiostat. The impedance measurements were carried out using a BAS-Zahner IM6 Impedance analyzer. The frequency range is from 100 mHz to 100 kHz. The cross-section of microbatteries was examined by field emission scanning electron microscopy (FE-SEM, LEO-1530 SEM system). The phase identification was carried out by x-ray diffraction (XRD, Philips X'Pert Pro Super X-ray diffractometer, Cu $K\alpha$ radiation, at a 2° min^{-1} scan rate). The electrochemical measurements of Al films deposited on Pt/SiO₂/Si substrates were performed with test coin cells which were assembled in an argon-filled glove box, and the electrolyte was a 1.0 M solution of LiPF₆ dissolved in a mixture of ethylene carbonate/ethylmethyl carbonate/diethyl carbonate (EC/EMC/DMC = 1:1:1).

3. Results and discussion

Figure 2 displays the top view photograph of the microbatteries on the silicon wafer. The current collector pads and morphology of the microbatteries are clearly seen. Figure 3 shows the SEM cross-sectional image of an as-deposited microbattery with the Al/LiPON/LiCoO₂/Pt construction. The thicknesses of LiCoO₂, LiPON and Al films were estimated to be 340, 610 and 150 nm, respectively, and the total thickness of this microscale battery is thus about 1.5 μm . The interfaces between the LiCoO₂ cathode, LiPON electrolyte and Al anode are smooth without any defects such as pinholes or cracks. The XRD patterns of LiCoO₂ films before and after annealing at 500 $^\circ\text{C}$ are presented in figure 4. The as-prepared LiCoO₂ films are amorphous, while the films after annealing at 500 $^\circ\text{C}$ exhibit (0 0 3) preferred orientation. Figure 5 shows the electrochemical performance of Al film in liquid electrolyte with Li metal as a counter electrode. At the first discharge process, there are two plateaus at 2.2 and 0.26 V, respectively. The plateau at 2.2 V is related to the reduction of aluminum oxide species on the surface of the aluminum film [27]. In the following cycles, the plateau at 0.26 V during the discharge process and at 0.44 V during the charge process can be assigned

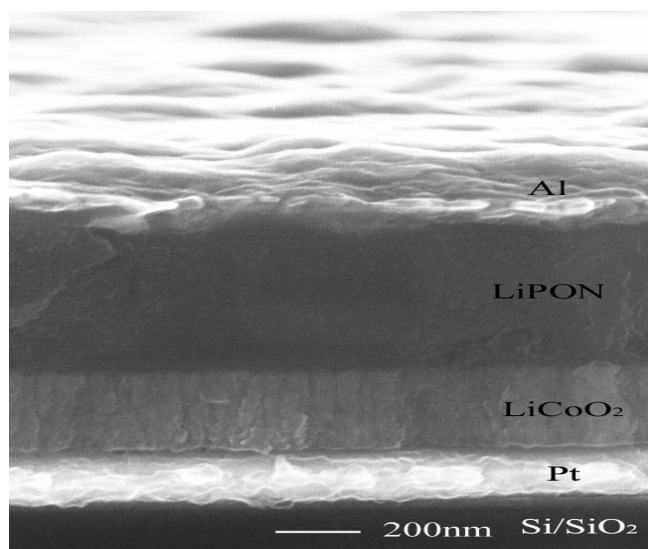


Figure 3. SEM image of the cross-section of the as-deposited microbattery.

to the alloying and dealloying processes of LiAl, respectively. The reversible capacity of the Al film decreases at the first cycle probably due to the formation of unreversible phases of LiAl. This result indicates that Al could be used as anode for lithium batteries [26, 27], but more studies are still needed to avoid the capacity loss at the first cycle.

Typical charge and discharge profiles for a single microbattery are shown in figure 6. During charging, there is a voltage plateau at about 3.3 V, which can be ascribed to the extraction of lithium from the LiCoO₂ cathode and the subsequent formation of active anode film at the interface between LiPON and Al films. The impedance results of the as-prepared microbattery and at different charge/discharge potentials are presented in figure 7. For the as-prepared cell, the impedance spectrum shows a behavior of blocking electrodes. A line was observed at low frequencies, which was followed by a semicircle in the high frequency range. After the cell is charged to 3.7 V, a new arc appears in the middle

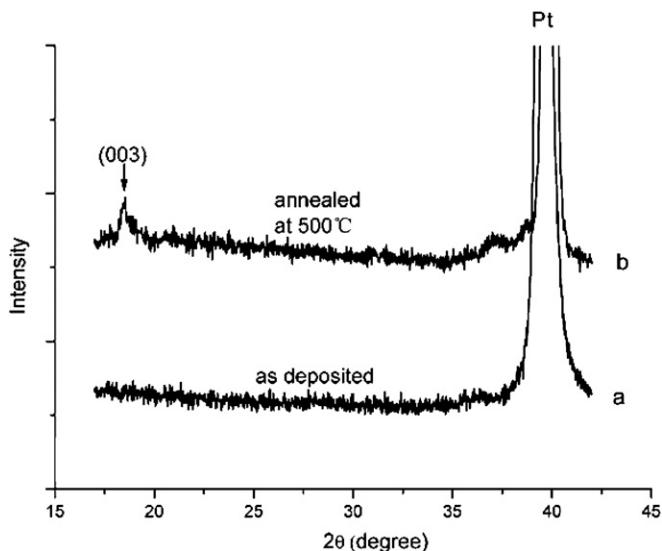


Figure 4. XRD patterns of LiCoO₂ thin films: (a) as-prepared, (b) annealed at 500 °C.

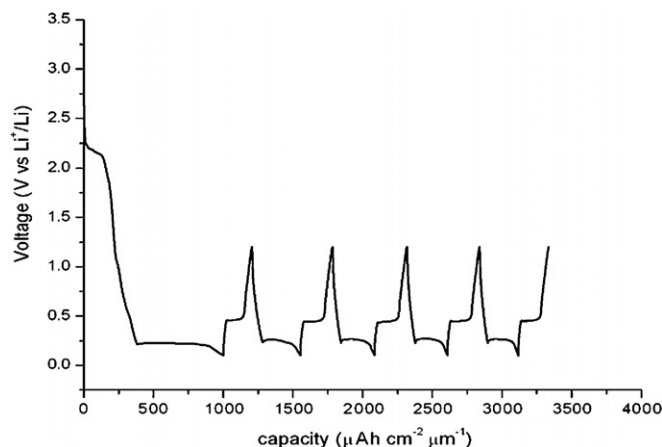


Figure 5. The charge and discharge curves of Al film at a current density of 10 μA cm⁻² in liquid electrolyte.

frequency range, which may imply a new phase formed at the interface between the solid electrolyte and Al films. This is possibly because the lithium ions are reduced to Li metal at the interface between aluminum and electrolyte and form a LiAl alloy at the charge step. The remnant aluminum films on top of the cells thus act as a current collector. When the cell is discharged to 1.5 V, the arc at the middle frequencies is not observed due to a change of LiAl anode to aluminum film. During the discharge process, lithium is oxidized from anode films and inserted into the cathode films, and a sloping voltage profile instead of a flat discharge curve was observed in figure 6. This is probably because the internal resistance of a microbattery is large due to the small area, low ionic conductivity of the solid-state electrolyte (in the order of 10⁻⁷ S cm⁻¹) and the interface resistance between the cathode and electrolyte. This will cause a large polarization when the battery is discharged. One solution for this problem is to use solid-state electrolyte with high ionic conductivity or some heat treatment to reduce the interface resistance [28].

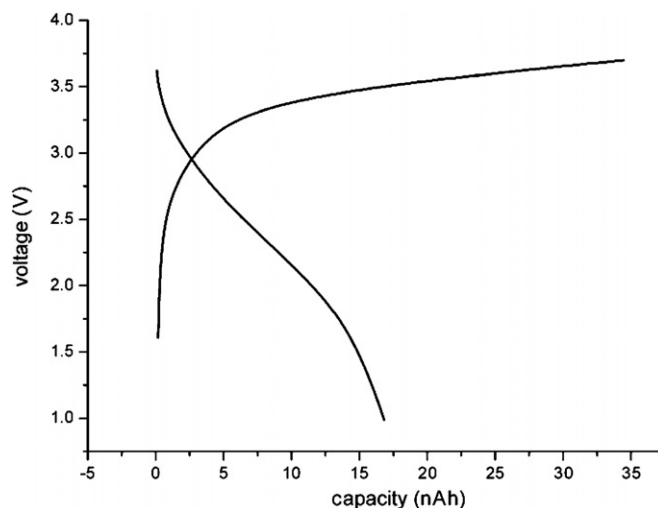


Figure 6. Typical charge and discharge curves of the microbatteries with the structure of Al/LiPON/LiCoO₂; the charge current is 10 nA, and the discharge current is 5 nA.

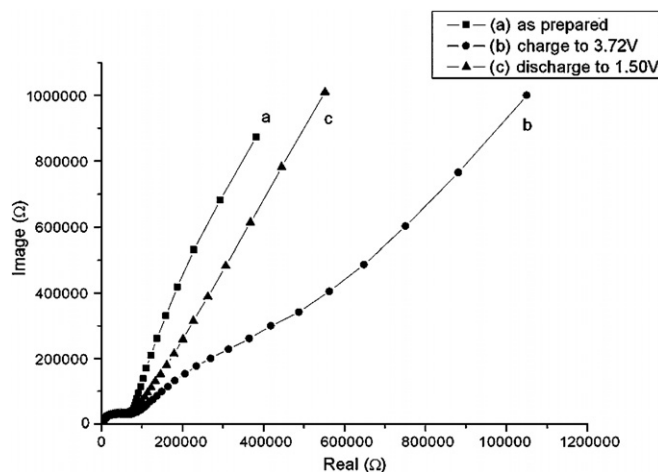


Figure 7. The impedance spectra of the microbattery for (a) as-deposited, (b) at a charge state of 3.72 V and (c) at a discharge state of 1.50 V versus Al/LiAl.

The theoretical capacity of the microbattery is about 29 nAh, calculated by the volumetric capacity of 35 μAh cm⁻² μm⁻¹ of LiCoO₂ films annealed at 500 °C. In our work, a single microbattery delivers a capacity of about 17 nAh in the initial cycles; it is comparable with the result reported by Whitacre *et al* [9], who used Li metal as the anode. The capacity loss may be ascribed to the initial irreversible loss at the LiAl alloy formation. We will try to use sputtered AlLi alloy films as anode instead of Al films in order to reduce the irreversible capacity.

The rate capability of the microscale lithium battery is shown in figure 8. The discharge capacity decreases with the rate. It is noticed that the microbattery is capable of sustaining the current of 40 nA, delivering 6.5 nAh reversible capacity in the voltage range of 1.0–4.0 V. At a current of 10 nA, the capacity during charging appears larger than that during discharge. We attribute this difference to a parasitic process such as moisture oxidation. The microbattery was cycled at

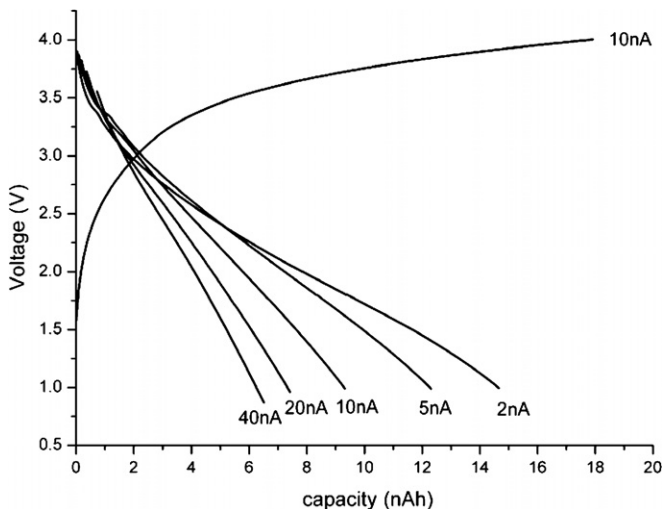


Figure 8. Rate capacity of an Al/LiPON/LiCoO₂ microbattery. The charge current of all rate capacity test was 10 nA, and the voltage range is 1.0–4.0 V.

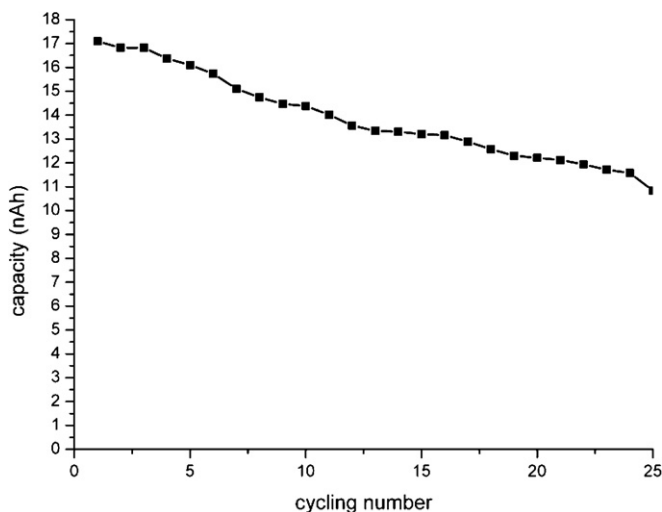


Figure 9. Cycling performance of an Al/LiPON/LiCoO₂ microbattery. The voltage range was 1.0–4.0 V, the charge current is 10 nA and the discharge current is 5 nA.

atmosphere at the discharge current of 5 nA, as shown in figure 9; after 25 cycles the microbattery delivers 63% of its initial capacity. One reason of the capacity loss is the alloy and dealloy processes of LiAl film at the anode. Another is due to the air and water leakage into the protective caps, causing the damage of the LiAl anode. Neudecker *et al* [4] reported that the thin-film battery with the parylene encapsulation resulted in decreased irreversible capacity and capacity fade. The long-term behavior of these microbatteries is currently under examination with an improved packing technique.

4. Conclusions

A microfabrication process of microscale lithium batteries was introduced, and photolithography, sputtering as well as wet etching techniques were employed in the fabrication

process. Al films were used for the first time as the anode and anode current collector in microscale lithium batteries. These microscale batteries with areas of the order of (500 μm)² deliver a capacity of 11–17 nAh at a 1/3C rate current, and can be operated at as high as 40 nA discharge current. Currently longer cycling life of the microbatteries was not obtained; we can expect good cycling performances of the microscale batteries with optimization of encapsulation. The improvements of energy density and cycling life of the microbatteries are under investigation in our groups. These microscale lithium batteries can be connected with micro solar cells to be micropower source systems with energy harvest and storage. These integrated micropower systems will be useful for providing on-chip power for microspacecraft and other microdevices.

Acknowledgments

The authors thank Zhongzi Luo and Chunquan Zhang for stimulating discussion and technical support. This work was supported by the National 973 Program (2009CB220102), the Basic Research Project of National Defence (XMDX2008176) and the Key Project founded by Fujian province (2006H0090).

References

- [1] Paul B, Koeneman IJB-V and Kristin L W 1997 Feasibility of micro power supplies for MEMS *J. Microelectromech. Syst.* **6** 355–62
- [2] Sammoura F, Lee K B and Lin L W 2004 Water-activated disposable and long shelf life microbatteries *Sensors Actuators A* **111** 79–86
- [3] Chamran F, Yeh Y, Min H S, Dunn B and Kim C J 2007 Fabrication of high-aspect-ratio electrode arrays for three-dimensional microbatteries *J. Microelectromech. Syst.* **16** 844–52
- [4] Yen T J, Fang N, Zhang X, Lu G Q and Wang C Y 2003 A micro methanol fuel cell operating at near room temperature *Appl. Phys. Lett.* **83** 4056–8
- [5] Jiang Y Q, Wang X H, Zhong L Y and Liu L 2006 Design, fabrication and testing of a silicon-based air-breathing micro direct methanol fuel cell *J. Micromech. Microeng.* **16** S233–9
- [6] Bieberle-Hutter A, Beckel D, Infortuna A, Muecke U P and Rupp J L M *et al* 2008 A micro-solid oxide fuel cell system as battery replacement *J. Power Sources* **177** 123–30
- [7] Cardenas-Valencia A M, Dlutowski J, Knighton S, Biver C J, Bumgarner J and Langebrake L 2007 Aluminum-anode, silicon-based micro-cells for powering expendable MEMS and lab-on-a-chip devices *Sensors Actuators B* **122** 328–36
- [8] Song J, Wu Q H, Dong Q F, Zheng M S, Wu S T and Sun S G 2007 Solid-state thin film Li-ion batteries *Prog. Chem.* **19** 66–73
- [9] Yu X H, Bates J B, Jellison G E and Hart F X 1997 A stable thin-film lithium electrolyte: lithium phosphorus oxynitride *J. Electrochem. Soc.* **144** 524–32
- [10] Dudney N J, Bates J B, Zuhr R A, Young S and Robertson J D *et al* 1999 Nanocrystalline Li_xMn_{2–y}O₄ cathodes for solid-state thin-film rechargeable lithium batteries *J. Electrochem. Soc.* **146** 2455–64
- [11] Choi C H, Cho W I, Cho B W, Kim H S, Yoon Y S and Tak Y S 2002 Radio-frequency magnetron sputtering power effect on the ionic conductivities of upon films *Electrochem. Solid State Lett.* **5** A14–7

- [12] Zhao S L, Fu Z W and Qin Q Z 2002 A solid-state electrolyte lithium phosphorus oxynitride film prepared by pulsed laser deposition *Thin Solid Films* **415** 108–13
- [13] Kim H K, Seong T Y and Yoon Y S 2003 Structural study of amorphous vanadium oxide films for thin film microbattery *J. Vac. Sci. Technol. B* **21** 754–9
- [14] Liao C L and Fung K Z 2004 Lithium cobalt oxide cathode film prepared by rf sputtering *J. Power Sources* **128** 263–9
- [15] Park H Y et al 2007 LiCoO₂ thin film cathode fabrication by rapid thermal annealing for micro power sources *Electrochim. Acta* **52** 2062–7
- [16] Bates J B, Dudney N J, Neudecker B, Ueda A and Evans C D 2000 Thin-film lithium and lithium-ion batteries *Solid State Ion.* **135** 33–45
- [17] Lee S J, Balk H K and Lee S M 2003 An all-solid-state thin film battery using LISIPON electrolyte and Si-V negative electrode films *Electrochem. Commun.* **5** 32–5
- [18] Nathan M et al 2005 Three-dimensional thin-film Li-ion microbatteries for autonomous MEMS *J. Microelectromech. Syst.* **14** 879–85
- [19] Kuwata N, Kawamura J, Toribami K, Hattori T and Sata N 2004 Thin-film lithium-ion battery with amorphous solid electrolyte fabricated by pulsed laser deposition *Electrochem. Commun.* **6** 417–21
- [20] Song J, Cai M Z, Dong Q F, Zheng M S, Wu Q H and Wu S T 2009 Structural and electrochemical characterization of SnO_x thin films for Li-ion microbattery *Electrochim. Acta* DOI: [10.1016/j.electacta.2008.11.026](https://doi.org/10.1016/j.electacta.2008.11.026)
- [21] West W C, Whitacre J F, White V and Ratnakumar B V 2002 Fabrication and testing of all solid-state microscale lithium batteries for microspacecraft applications *J. Micromech. Microeng.* **12** 58–62
- [22] Neudecker B J, Dudney N J and Bates J B 2000 'Lithium-free' thin-film battery with in situ plated Li anode *J. Electrochem. Soc.* **147** 517–23
- [23] Whitacre J F, West W C and Ratnakumar B V 2003 A combinatorial study of Li_yMnxNi_{2-x}O₄ cathode materials using microfabricated solid-state electrochemical cells *J. Electrochem. Soc.* **150** A1676–83
- [24] Notten P H L, Roozeboom F, Niessen R A H and Baggetto L 2007 3-D integrated all-solid-state rechargeable batteries *Adv. Mater.* **19** 4564–7
- [25] Baggetto L, Niessen R A H, Roozeboom F and Notten P H L 2008 High energy density all-solid-state batteries: a challenging concept towards 3D integration *Adv. Funct. Mater.* **18** 1057–66
- [26] Schwenzel J, Thangadurai V and Weppner W 2003 Investigation of thin film all-solid-state lithium ion battery materials *Ionics* **9** 348–56
- [27] Hamon Y, Brousse T, Jousse F, Topart P, Buvat P and Schleich D M 2001 Aluminum negative electrode in lithium ion batteries *J. Power Sources* **97** 185–7
- [28] Iriyama Y, Kako T, Yada C, Abe T and Ogumi Z 2005 Charge transfer reaction at the lithium phosphorus oxynitride glass electrolyte/lithium cobalt oxide thin film interface *Solid State Ion.* **176** 2371–6